Broadband and polarization-selective optical switch in infrared spectrum based on SMT materials

Zhang Xuanru[1], Wang Wei[2], Xiang Bin[2], Lu Yalin[1,2]

(1. Advanced Applied Research Center, Hefei National Laboratory for Physical Science at the Microscale, University of Science and Technology of China, Hefei 230026, China;
2. CAS Key Laboratory of Materials for Energy Conversion, Department of Material Science and Engineering, University of Science and Technology of China, Hefei 230026, China)

Abstract: A new design of optical switch composed of a vanadium dioxide(VO_2) thin film and embedded sub-wavelength metallic gratings was proposed. The numerical calculations of the device performance were carried out using the Finite Element Method (FEM). This design exhibited broadband and polarization selective all-optical switching effects in the near-infrared spectrum. The embedded gratings enhanced the extinction ratio of the VO_2 film, and achieved high extinction ratio in sub-wavelength device size. The optical properties of the proposed design depended little on the incident angle. In addition, the transmittance and absorbance can be tuned by the geometric parameters. The device has great potential usages as the infrared spectrum is of great important both in optical communication and computering, and optical imaging in military reconnaissance and industrial non-destructive detecting.

Key words: semiconductor-metal transition material; broadband optical switch; embedded gratings
CLC number: O439 **Document code:** A **Article ID:** 1007-2276(2014)09-2787-06

基于半导体-金属相变材料的宽谱、偏振选择的红外光开关

张璇如[1],王 威[2],向 斌[2],陆亚林[1,2]

(1. 中国科学技术大学 合肥微尺度物质科学国家实验室(筹) 应用科学研究中心,安徽 合肥 230026;
2. 中国科学技术大学 材料科学与工程系 中国科学院能量转换材料重点实验室,安徽 合肥 230026)

摘 要: 提出了一种基于半导体-金属相变材料和掩埋金属光栅结构的新型红外光开关。该结果由电磁场有限元方法计算得到。设计了在近红外波段表现出宽谱的、偏振选择的全光开关效应。掩埋金属光栅极大的提高了二氧化钒薄膜作为光开关的消光比,使得该结构在亚波长尺寸获得了高的消光比。结构的光学响应随入射角变化并不敏感。结构的透过、吸收特性可由结构参数进行调节。此设计在红外光通信、光计算以及军事探测、无损检测等领域具有潜在的应用。

关键词: 半导体-金属相变材料; 宽谱光开关; 掩埋光栅

收稿日期:2014-01-05; **修订日期:**2014-02-03

基金项目:国家重点基础研究发展计划(973 计划)(2012CB922000)

作者简介:张璇如(1987-),女,博士生,主要从事表面等离激元方面的研究。Email:zhangxru@mail.ustc.edu.cn

导师简介:陆亚林(1964-),男,教授,主要从事光电功能材料和器件方面的研究。Email:yllu@ustc.edu.cn

0 Introduction

Optical information processin g has advantages over the electronic technology, such as high speed, large bandwidth, ease of noninterfering parallelism, etc[1]. In future optical networks, optical switches are essential elements, just as electrical switches in electrical circuits. A feasible optical switch should have high extinction ratio, fast switch speed and low threshold[2]. Besides, small device size is also expected for integration. We also expect incident angle-insensitive performance, for easy alignment. And under different usage situations, we may want polarization-selective or polarization-insensitive devices. Sometimes we want the device working at single wavelength, and sometimes we want it to work in a wide spectrum.

There are many kinds of means to control the on and off of the optical switches, such as mechanical, electrical and all-optical. Mechanical optical switches are the oldest and mostly widely used ones. These devices achieve switching via moving of the optical elements by means of step motors or relay arms. They can achieve excellent reliability and insertion loss, but with slow reactive time in 10−100 ms range. Thermal, electrical or all-optical switches usually employs materials, refractive index of which will change under excitations of thermal, electrical or optical[2−4]. These switches often combine these refractive-change materials with optical resonant structures, such as micro cavities. The refactive index change caused by the excitation results in the shift of the structure′s resonant wavelength, as the on and off at certain wavelength. However, the structure and fabrication process of these switches are relatively complex, and most of them work at single working wavelength.

To achieve broad working spectrum, optical switches based on VO_2 were introduced. VO_2 exhibited a fast, reversible first-order Semiconductor-Metal Transition (SMT) via different external excitations, such as thermal excitation, electrical excitation, or optical excitation[5−9]. During SMT, VO_2 experiences a structural adjustment from the monoclinic phase to the rutile phase. It′s transparent in the semiconductive phase but highly reflective and absorptive in the metallic phase, in the infrared (IR) spectrum. The SMT could occur within 500 fs[10]. It′s also reported that the VO_2 thin films can survive the stress during 108 cycles of SMT[11]. The special characters ensure the VO_2 thin films as fast optical switch, at wide IR spectrum. Much research has been tried to enhance VO_2 film extinction ratio, through fabrication method improvement or doping[12]. However, it has little real impact.

With the developing of nano-fabrication, metallic gratings are easy to industrial production and widely used in kinds of devices. For example in solar cells, adding an embedded metallic grating can enhance the absorption in a wide spectrum[13]. In this paper, we combine embedded metallic gratings and VO_2 films together, expecting it will have improvement. Via simulations, we show that our proposed structure exhibits broadband and polarization-selective optical switching in infrared. The device is at sub-wavelength scale, and the optical properties depend little on the incident angle. Besides, the transmittance can be tuned by geometric parameters. As VO_2 can exhibit the SMT via different kinds of external excitation, our design is instructive and meaningful in thermal, electrical and all-optical switches. The device has great potential usages as the infrared spectrum is of great important both in optical communication and computering, and optical imaging in military reconnaissance and industrial non-destructive detecting. The polarization-selective property makes our design useful in infrared polarimetry imaging[14−15].

1 Computational methods

Figure 1 shows the side view of the proposed structure. Silver gratings were at the bottom of the VO_2 film, with the grating slits filled with VO_2. The

period, thickness, and width of the Ag grating are p, t_1, and w, respectively. The thickness of the VO_2 layer is t_2. The structure is deposited on a K9 glass substrate. The signal light illuminates from the top side.

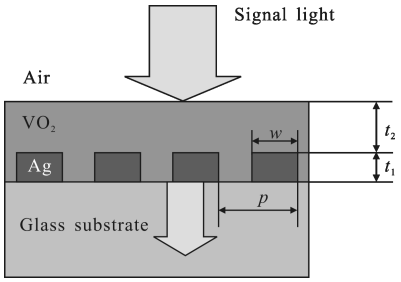

Fig.1 Schematic view of the proposed structure

We use commerci ally available 2 -dimensional (2D) finite element method (FEM) software (Comsol 3.3a) for our simulation. The computational domain considered is a single unit cell surrounded by periodic boundary conditions[16]. For this study, we consider the spectra from 350 nm to 5 μm, from visible to IR. The dielectric constant of silver is taken from tabulated data in Ref. [17]. The dispersion of the K9 glass is very small, which we neglect. The refractive index of the K9 glass is treated as a constant 1.51. The dielectric constant of semiconductive phase VO_2 is taken from interpolating of the experimental data from Ref. [18], while the metallic VO_2 is modeled in a Drude form Ref.[19].

2 Results and discussions

2.1 The broadband and polarization-selective all-optical switching effect

Figure 2 shows the transmittance (dotted line, denoted as ´*T*´) and absorbance (solid line, denoted as ´*A*´) for semiconductive (a) and metallic (b) phase VO_2, with p=200 nm, t_1=100 nm, t_2=150 nm, w=100 nm. The incidence is assumed to be at normal. We focus on transmittances first. For the semiconductor phase, the switch is at the ´on´ state. It exhibits a broadband transmission in the broad infrared spectrum (>2 μm) for TM waves, and nearly zero transmittance for TE waves. Using the switch as a polarization-splitter, the TE waves can be reflected while the TM waves can be transmitted. For metallic phase, the switch is ´off´. It cuts off for both polarizations in infrared. Thus, our structure acts as a broadband, polarization-selective switch in the infrared range.

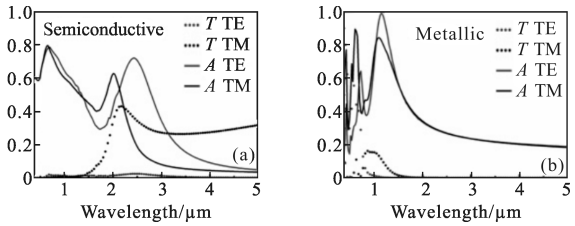

Fig.2 Transmittance and absorbance of our structure for semiconductive (a) and metallic (b) VO_2

For absorbance analysis, waves of both polarizations exhibit high absorbance in the visible and near-infrared spectrum(<1.5 μm), with both semiconductor and metallic phase VO_2. This is caused by the high absorption of VO_2 in this spectrum. There are absorption peaks of different shapes in the region <2 μm. These are the cooperating results of the materials′ dispersion and the cavity resonance. For switches worked under optical excitation, we can fix the pump wavelength in this high absorbing region, as the high absorbance ensures a fast switching speed and a low threshold. The pump light can be either homochromatic or broadband.

The total thickness of our structure is 250 nm, and the grating period is 200 nm; both are much smaller than the working wavelength. Sub-wavelength size is always expected in integrated photonics.

2.2 Explanations of the effective medium theory

The broadband and polarization-selective transmission can be explained by the Effective Medium Theory(EMT). When un-polarized EM waves incident on the deeply sub-wavelength metallic grating, the electromagnetic field oscillating parallel to the wires (TE waves) generates electron movement along the wires in response to the oscillating field[15,20-21]. Since the electrons are free to move in this direction and the wire width is much smaller than the incident

wavelength, the polarizer behaves in a similar manner to the surface of a metal when reflecting light, with losses due to Joule heating (Fig.3 (c)). On the other hand, EM waves oscillating perpendicularly to the wires (TM waves) is not in the same way which is able to induce electron movement. Therefore, the loss due to Joule heating and reflection is limited, the grating acts as dielectric film and the wave transmits through the grating(Fig.3(a)). As we want broadband working spectrum here, the grating depth and period should be much smaller than the wavelength. However, the thickness of the grating must be larger than the evanescent length in the metal, to block the TE waves. Extending the grating size comparable with the signal wavelength can introduce new physical effects such as longitude Fabry-Perot (FP) resonance in the grating slit [22], and Surface Plasmon Polaritons(SPPs) at the interface of the metal and VO_2[23].

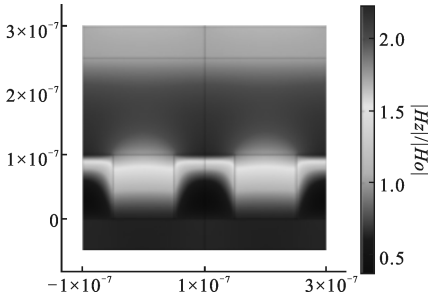

(a) 3 μm TM wave

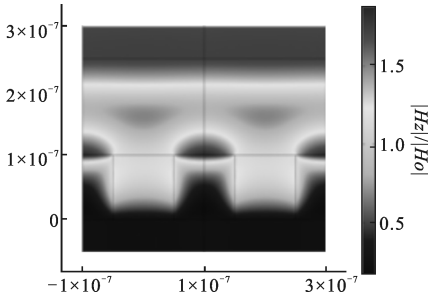

(b) 1 μm TM wave

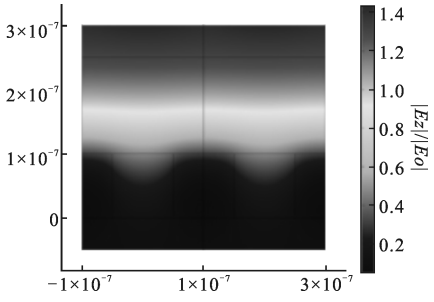

(c) 3 μm TE wave

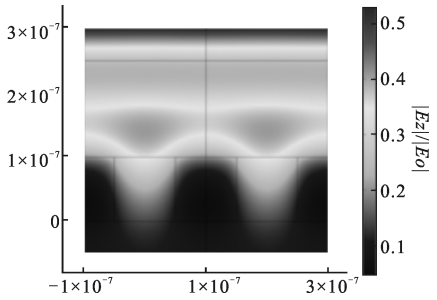

(d) 1 μm TE wave

Fig.3 Normalized and time-averaged field plots across the structure

These resonant effects can enhance the performance at the resonant peak, but limit the working spectrum. These are left for further discussion.

At shorter wavelength regime, the EMT still holds, but other effects participate in. Because of the scattering of the TM waves, the Surface Plasmon Polaritons (SPPs) enhance the local electromagnetic field thus the absorption of the TM waves (Fig.3(b)). For both polarizations, the FP resonance occurs when is <2 μm in the semiconductive VO_2 layer (Fig.3(b), (d)). The FP effect cooperates with the materials′ dispersion, leading to several peaks. The total cut-off of both polarizations at the visible and near-infrared spectrum results from the strong absorption of VO_2.

Under the approximation of EMT, the grating layer acts as a uniform layer with effective dielectric constants (Fig.4(e)). The effective complex refractive index of the deeply sub-wavelength binary grating of filling-factor f_1 for medium 1 and filling-factor f_2 for medium 2 is:

$$n_{TE}=[f_1(n_1+ik_1)^2+f_2(n_2+ik_2)^2]^{1/2}$$

$$n_{TM}=[f_1(n_1+ik_1)^{-2}+f_2(n_2+ik_2)^{-2}]^{-1/2} \quad (f_1+f_2=1)$$

The effective n and k of the embedded binary grating composed of Ag and VO_2 (only the grating layer of thickness t_1, without the top VO_2 layer) are shown in Fig.4 (a) and (b). The effective index of TM waves acts similar to that of semiconductive VO_2, while those of TE waves are like Ag′s. These coincide with aforementioned physical explanations. We also compare the transmission results obtained by FEM and EMT. The peaks in the EMT are coincident well with those in the FEM result, while the amplitudes are slightly different. We can design and

optimize the structure more conveniently in the EMT, and confirm it in FEM.

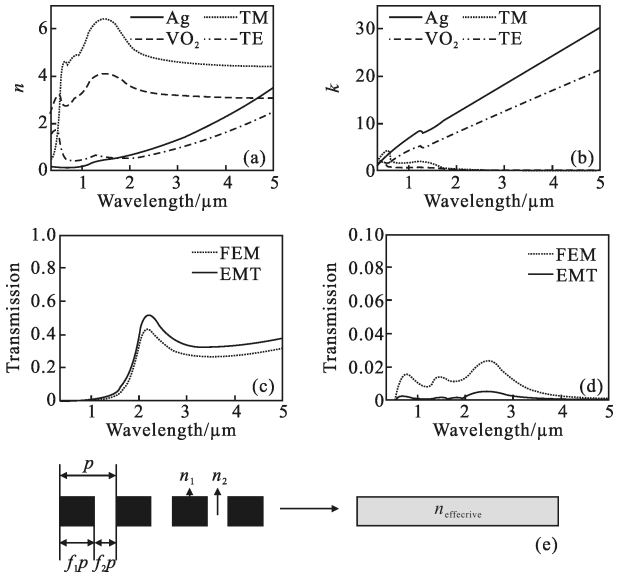

Fig.4 (a) and (b) the effective n and k for both polarizations, compared with Ag and semiconductive VO2. (c) and (d) transmission results for semiconductive VO2 obtained by the FEM and EMT, with (c) for TM waves and (d) for TE waves. (e) The effective medium approximation of the grating structure.

2.3 Dependence on the geometric parameters

Now we will tune the geometric parameters, and discuss the dependence of the transmission on them. We study the effects of the thickness of the grating t_1(Fig.5) and the thickness of the top VO_2 layer t_2(Fig.6).

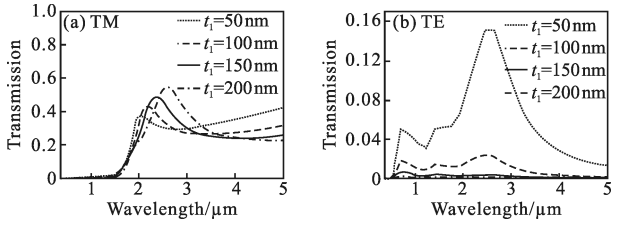

Fig.5 Transmission spectrums with varying grating′s thicknesses t_1, fixing the top layer thickness t_2 and other structural parameters

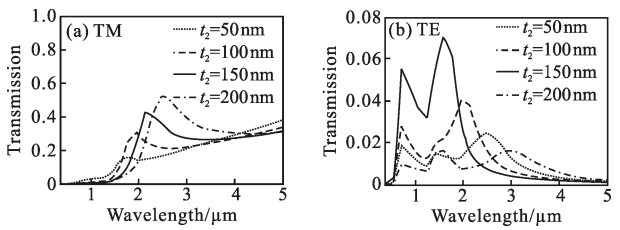

Fig.6 Transmission spectrums versus the VO_2 layer thickness t_2, with other structural parameters fixed

The transmission peaks of TM waves at about 2 μm red shift with both increasing t_1 and t_2. It corresponds to the FP resonance peak of TM waves. From EMT, the grating layer acts as dielectric, and participates in the FP cavity. So the peak shifts with both t_1 and t_2.

The geometry parameters of the grating, yet the fill factor and the grating period, also affect the performance (Fig.7). However, they do not affect the peak position. The filling factor affects the amplitude, as it affects the effective dielectric constants. However, the dependence on the grating period will be complex with larger periods out of the EMT regime.

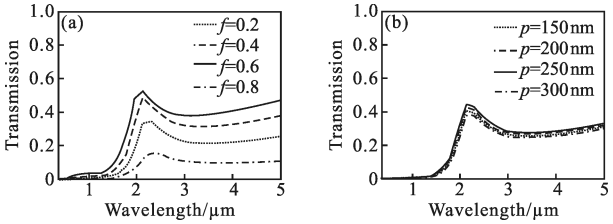

Fig.7 Transmission for TM waves, with varying fill factors of Ag (a) and grating thicknesses (b).

2.4 Dependence on the incident angle

The alignment problem is always annoying in photonic devices, and above discussions are for normal incidence. Finally we consider the dependence of our device on the incident angle. As shown in Fig.8, the transmittance and absorbance depend little on the incident angle (i.e., the horizontal wave vector k_x). That′s because it′s in the air where the light illuminates. The semiconductor-phase VO_2 has a refractive index about 3.5. From Fresnel equations, the refractive angle in the VO_2 is 0°−16°, corresponding to 0°−90°incident angle in air[22]. It means that the proposed device design is alignment-free, which is expected for an optical or photonic device.

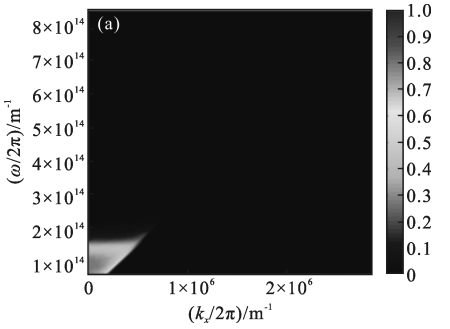

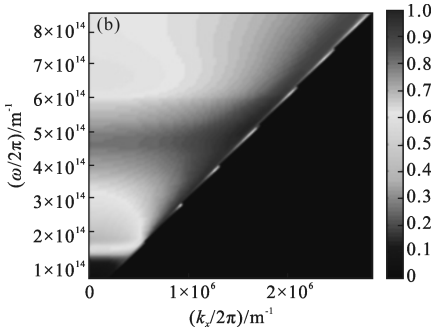

Fig.8 Contour plot of transmittance (a) and absorbance (b) in the $\omega-k_x$ domain, for TM waves, with p=200 nm, t_2=100 nm, w=100 nm, t=250 nm

3 Conclusion

In conclusion, we num erically demonstrated a broadband and polarization-selective optical switch in the infrared spectrum, based on thin films of SMT material VO_2 and embedded sub-wavelength metallic gratings. Its transmission and absorption properties are investigated. This switch achieves an extinction ratio of 550:1. The size of the structure is in the sub-wavelength scale. Besides, the device exhibits little dependence on the incident angle. The transmittance and absorbance can be tuned by the geometric parameters.

References:

[1] Yariv A. Quantum Electronics [M]. New York: John Wiley, 1989.

[2] Gibbs H M. Optical Bistability: Controlling Light with Light [M]. Pittsburgh: Academic Press, 1985.

[3] Chen J, Wang P, Wang X, et al. Sensitivity enhanced all-optical switching using prism-grating coupled surface plasmon modes [J]. ***Optics Communications***, 2010, 283: 151–154.

[4] Wang X, Jiang H, Chen J, et al. Optical bistability effect in plasmonic racetrack resonator with high extinction ratio [J]. ***Optics Express***, 2011, 19: 19415–19421.

[5] Morin F J. Oxides which show a metal-to-insulator transition at the Neel temperature[J]. ***Physical Review Letters***, 1959, 3: 34–36.

[6] Kang L, Gao Y, Luo H. A novel solution process for the synthesis of VO_2 thin films with excellent thermochromic properties [J]. ***Acs Applied Materials & Interfaces***, 2009, 1: 2211–2218.

[7] Yan J, Huang W, Li N. Structure and infrared optical properties of VO_2/TiO_2 multilayer film [J]. ***Infrared and Laser Engineering***, 2013, 42 (9): 2485. (in Chinese)

[8] Lu Y, Ling Y, Feng Y, et al. Analysis of VO_2 thin film intelligent protection against pulsed power infrared-laser [J]. ***Infrared and Laser Engineering***, 2012, 41(11): 2886. (in Chinese)

[9] Liu D, Cheng H, Zheng W, et al. Applications of VO_2 in adaptive infrared stealth technology [J]. ***Infrared and Laser Engineering***, 2012, 41(11): 2898. (in Chinese)

[10] Cavalleri A, Toth C, Siders C W, et al. Femtosecond structural dynamics in VO_2 during an ultrafast solid-solid phase transition[J]. ***Physical Review Letters***, 2001, 87: 237401.

[11] Beteille F, Livage J. Optical switching in VO_2 thin films [J]. ***Journal of Sol–Gel Science and Technology***, 1998, 13: 915–921.

[12] Guinneton F, Sauques L, Valmalette J C, et al. Optimized infrared switching properties in thermochromic vanadium dioxide thin films: role of deposition process and microstructure [J]. ***Thin Solid Films***, 2004, 446: 287–295.

[13] Wang W, Wu S, Reinhardt K, et al. Broadband light absorption enhancement in thin-film silicon solar cells [J]. ***Nano Letters***, 2010, 10: 2012–2018.

[14] Tyo J S, Goldstein D L, Chenault D B, et al. Review of passive imaging polarimetry for remote sensing applications [J]. ***Applied Optics***, 2006, 45: 5453–5469.

[15] Kang G G, Tan Q F, Chen W L, et al. Design and fabrication of sub –wavelength metal wire-grid and its application to experimental study of polarimetric imaging [J]. ***Acta Physica Sinica***, 2011, 60: 014218.

[16] Jin J. The Finite Element Method in Electromagnetics [M]. New York: Wiley, 2002.

[17] Palik E D. Handbook of Optical Constants of Solid [M]. Pittsburgh: Academic Press, 1985.

[18] Gavini A, Kwan C C Y. Optical properties of semiconducting VO_2 films [J]. ***Physical Review B***, 1972, 5: 3138–3143.

[19] Xiao D, Kim K W, Zavada J M. Electrically programmable photonic crystal slab based on the metal-insulator transition in VO_2 [J]. ***Journal of Applied Physics***, 2005, 97: 106102.

[20] Richter I, Sun P C, Xu F, Satto M, Design considerations of form birefringent microstructures [J]. ***Applied Optics***, 1995, 34: 2421–2429.

[21] Yamada I, Nishii J, Saito M. Modeling, fabrication, and characterization of tungsten silicide wire-grid polarizer in infrared region [J]. ***Applied Optics***, 2008, 47: 4735–4738.

[22] Wolf E, Born M. Principles of Optics: Electromagnetic Theory of Propagation, Interference and Diffraction of Light [M]. Cambridge: Cambridge University Press, 1999.

[23] Barnes W L, Dereux A, Ebbesen T W. Surface plasmon subwavelength optics[J]. ***Nature***, 2003, 424: 824–830.